ELSEVIER

Polymer 43 (2002) 7443–7450

polymer

www.elsevier.com/locate/polymer

Phase distribution and separation in poly(2-acetoxyethyl methacrylate)/polystyrene latex interpenetrating polymer networks

S. Shi, S. Kuroda*, S. Tadaki, H. Kubota

Department of Chemistry, Faculty of Engineering, Gunma University, 1-5-1 Ten'jin-cho, Kiryu, Gunma 376-8515, Japan

Received 19 June 2002; received in revised form 2 September 2002; accepted 9 September 2002

Abstract

A series of latex interpenetrating polymer networks (LIPNs) were prepared via two-stage soap-free emulsion polymerization of styrene on cross-linked poly(2-acetoxyethyl methacrylate) (PAEMA) seed latexes, using potassium persulfate as initiator. It was found that a compositional gradient was present when PAEMA seeds cross-linked either lightly or highly were used. The polystyrene (PS) phase is localized near the particle center in the former case, while it is segregated near the surface in the latter case. A uniform distribution of PS phase in LIPN was formed, if moderately cross-linked PAEMA seed was used. All the LIPNs appeared to be microphase-separated, and increase of cross-linking degree in seed latexes decreased the PS-rich domain size. The results were explained by the particle growth mechanism that involved the formation of surface-active oligomeric radicals in water phase, adsorption of the radicals onto monomer-swollen particle/water interface, and chain propagation in the interface with subsequent phase migration dominated by the competitive effects of thermodynamics and kinetics.

Keywords: Latex interpenetrating polymer network; Phase distribution; Phase separation

1. Introduction

Differing from the bulk interpenetrating polymer networks (IPN), latex IPN (LIPN) can be processed by using the compression molding, injection molding, painting or casting techniques since the thermosetting character is restricted within the latex particles usually ranging from several tens to a few hundreds of nanometers in diameter [1–5]. Due to the advantage in processibility, LIPN has been extensively investigated during the past few decades. LIPN is generally prepared via two-stage emulsion polymerization technique and a wide variety of factors involved in synthetic details influence, both thermodynamically and kinetically, the ultimate morphology of the resulting LIPN, thus rendering the control of morphology a significantly complicated subject. These factors include compatibility of constituent polymers [6–8], hydrophilicity [9], addition mode of second-stage monomer [10,11], composition [10,12–15], level of cross-linking in either first- or second-stage polymer [16–20], polymerization sequence [14,16,21], initiator type [12,18], and so on. Empirical summaries of the various possible morphologies resulted from the two-stage emulsion polymerization were given by Lee et al. [9] and Nemirovski et al. [22].

Among the factors controlling the morphology of LIPN, the compatibility between constituent polymers is of particular importance. In our laboratory, we have been interested in synthesizing the microphase-separated hydrophilic/hydrophobic IPN composed of poly(2-hydroxyethyl methacrylate) (PHEMA) and polystyrene (PS) because of its potential applications as biomedical materials [23]. However, the solubility parameters of PHEMA and PS are 23.0 [6] and 18.6 $(MPa)^{1/2}$ [24], respectively. For the polymer pair between which no specific intermolecular interactions are present, such great difference in solubility parameters undoubtedly means a complete incompatibility and full phase separation would be expected [6,25], if ordinary polymerization technique is employed. However, bulk sequential IPN (SIPN) consisting of this highly incompatible polymer pair was successfully synthesized in the presence of a common solvent, which is capable of swelling the first-stage polymer network and, at the same time, dissolving the second-stage monomer. The phase separation was limited to, at the minimum, tens of nanometers [26,27]. On the other hand, we have also designed an indirect

* Corresponding author. Tel.: +81-277-30-1375; fax: +81-277-30-1371.
E-mail address: skuroda@chem.gunma-u.ac.jp (S. Kuroda).

0032-3861/02/$ - see front matter
PII: S0032-3861(02)00683-3

Table 1
Recipes for the preparation of PAEMA seed latexes

Ingredients	AX0[a]	AX0.5[b]	AX1.0[b]	AX4.0[b]
AEMA (ml)	15	15	15	15
EGDMA (mol%)[c]	0	0.5	1.0	4.0
KPS (mg)	15	15	15	15
Water (ml)	150	450	450	450

[a] 300 ml separated flask was used; the agitator was 10 mm from the bottom of the flask.
[b] 500 ml separated flask was used; the agitator was 15 mm from the bottom of the flask.
[c] Based on the amount of AEMA monomer.

synthesis procedure in which the poly(2-acetoxyethyl methacrylate)(PAEMA)/PS LIPN having microphase-separated structure was first prepared as a precursor and it was hydrolyzed in aqueous KOH solution to obtain the LIPN with microphase-separated surface of hydrophilic/hydrophobic PHEMA/PS. More interestingly, this characteristic procedure also allowed the production of latexes with identical particle size and size distribution but different chemical structures and thus different chemical properties on the surface [28,29].

In this paper, we will describe the preparation of this microphase-separated PAEMA/PS LIPN with emphasizing how to control the morphology. A plausible particle growth mechanism was then proposed to elucidate the morphological development of the LIPN from the perspectives of thermodynamics and kinetics. In view of its potential applications in biochemical field, we conducted polymerization, for both the first- and second-stage, using a soap-free emulsion polymerization technique [30] to avoid contamination of the resultant latex particles by surfactant. A water-soluble initiator, potassium persulfate (KPS) was utilized.

2. Experimental

2.1. Materials

All reagents used in this study were purchased from Wako Pure Chemical Industries, Ltd, Japan. Styrene (Wako Special Grade) was washed repeatedly with 10% aqueous NaOH solution and deionized water, dried over anhydrous $NaSO_4$, and finally distilled under a reduced pressure of nitrogen. The inhibitor-free styrene was stored under nitrogen at about $-10\,^{\circ}C$ until used. 2-Hydroxyethyl methacrylate (HEMA, Wako 1st Grade) and ethylene glycol dimethacrylate (EGDMA, Wako 1st Grade) were purified by distillation under reduced pressure in a nitrogen atmosphere. AEMA monomer was synthesized by an esterification of HEMA with acetic anhydride, in the presence of pyridine as solvent and copper (II) chloride dihydrate as polymerization inhibitor [31]. KPS (Wako 1st Grade) was recrystallized from deionized water and stored in a refrigerator. KPS was used for polymerization within two weeks after recrystallization. Other reagents were used as received.

2.2. Preparations of PAEMA seed latexes and PAEMA/PS LIPNs

Hereafter, we use the following abbreviations to represent compositions of the seed and LIPN samples: A, X and S denote PAEMA, cross-linker of PAEMA, and PS, respectively. Numerals following X and S are the degree of cross-linking (mol%, based on AEMA monomer) and the amount of styrene (ml) added to the seed latex in the second-stage polymerization, respectively.

PAEMA seed latexes were prepared using a soap-free emulsion polymerization technique, in a 300 or 500 ml four-neck, round-bottom separated flask equipped with a nitrogen inlet, a syringe for sampling and a mechanical marine-type agitator (three-blade, ϕ50 mm). A typical synthesis was carried out in the following manner. Deionized water, AEMA monomer and its cross-linker (if used), EGDMA, were first charged to the flask and purged with nitrogen for 30 min with the vigorous agitation of 700 rpm to remove the dissolved oxygen. Then, the agitation speed was reduced to 300 rpm and KPS was added to the reaction mixture. The soap-free emulsion polymerization was carried out at $70 \pm 1\,^{\circ}C$ for 5 h, which usually achieved 95% or more monomer conversion. The milky-white latex solution, after removal of coagulum by filtration, was purified by dialysis against deionized water for 3 days, using well-washed seamless cellulose tubing. The dialysate was changed every 12 h. The details of the first-stage polymerization are given in Table 1.

PAEMA/PS LIPNs were prepared by the second-stage soap-free emulsion polymerization of styrene in the presence of PAEMA seed latexes, in a 300 ml separated flask identical with that used for seed preparation. An appropriate amount of PAEMA seed latex was charged to the flask and diluted to 130 ml with deionized water, then purged with nitrogen for 30 min with stirring constantly at 300 rpm. A required amount of oxygen-free styrene was added under nitrogen atmosphere after introduction of KPS initiator. Then as soon as possible, the reaction system was sealed after stopping the nitrogen flow and polymerization was initiated. The second-stage polymerization was carried out at $70 \pm 1\,^{\circ}C$ for 16 h. The details of the second-stage polymerization are given in Table 2.

2.3. Characterization

2.3.1. Dynamic light scattering (DLS)

The particle size and size distribution of latexes were determined by DLS using a commercial LPA-3100 spectrometer (Otsuka Electronics Co., Ltd) equipped with He–Ne laser operating at 632.8 nm. All measurements were carried out at $21.5\,^{\circ}C$ at a fixed angle of $90\,^{\circ}$ on highly

Table 2
Recipes for the preparation of PAEMA/PS LIPNs

LIPNs	Ingredients						
	AX0 (ml)	AX0.5 (ml)	AX1.0 (ml)	AX4.0 (ml)	Water (ml)	Styrene (ml)	KPS (mg)
AX0S1.2	5.8	–	–	–	124.2	1.2	10
AX0.5S1.2	–	18.3	–	–	111.7	1.2	10
AX1.0S1.2	–	–	20.7	–	109.3	1.2	10
AX4.0S1.2	–	–	–	25.5	104.5	1.2	10
AX1.0S0.4	–	–	20.7	–	109.3	0.4	10
AX1.0S3.0	–	–	20.7	–	109.3	3.0	10

The distance between the agitator and flask bottom was kept constant as 10 mm, all seed latexes used were adjusted to contain 0.55 g of the solid polymer.

diluted emulsion solution. Data analysis was made with the histogram method.

2.3.2. Fourier transform (FT)-IR spectroscopy

FT-IR spectra were obtained on a FT/IR-8000 spectrometer (Jasco) using the pressed-KBr-pellet technique. The specimens for the measurements, with a diameter of 3 mm, were prepared using a Micro KBr Pellet Die (Jasco Parts Center). The freeze-dried latex particles were used for IR analysis.

2.3.3. X-ray photoelectron spectroscopy (XPS)

XPS analysis was performed on a Perkin–Elmer ESCA 5600 spectrometer with an Mg Kα X-ray source (1253.6 eV) that was operated at an anode voltage of 15 kV and anode power of 400 W. Pass energies of 187.85 and 58.70 eV with corresponding energy step of 1.60 and 0.25 eV were used for the survey and multi-measurements, respectively. All the measurements were made with an analysis area of approximately 800 μm in diameter and at a take-off angle of 45 °. The pressure in the analysis chamber was kept at an order of 10^{-8} Torr or lower during the measurements. The atomic ratios of oxygen to carbon were determined from peak-area ratios, after correcting with the appropriate sensitivity factors provided by the instruments manufacturer (O, 41.068; C, 17.059). The freeze-dried LIPNs particles were used for XPS measurements.

2.3.4. Transmission electron microscopy (TEM)

The latexes prepared were washed repeatedly by centrifugation, coagulated and finally vacuum-dried at ambient temperature. Two or three pieces of the dried solid chips were embedded in epoxy (EPON 812 resin kit, TAAB) and then the epoxy was cured at 60 °C for 24 h. The cured blocks were trimmed and microtomed using the ultramicrotome supernova (JEOL, JUM-7). The obtained ultrathin cross-sections (ca. 60 nm in thickness) were carefully collected on a carbon-coated micro grid, dried in open air, and exposed to the ruthenium tetraoxide (RuO_4) vapor for 3 h at 25 °C. The RuO_4 staining solution was generated by the oxidation of hydrated ruthenium dioxide ($RuO_2{\cdot}x\,H_2O$) with an excess of aqueous sodium periodate ($NaIO_4$) solution, according to the method reported by Trent [32]. The RuO_4-stained ultrathin cross-sections were viewed to study the internal morphology of LIPN particles on a JEM-1200EXII microscope (JEOL) at an accelerating voltage of 80 kV. The transmission electron micrographs taken were digitized using a Cannon N1240U scanner at a resolution of 600 dpi.

3. Results and discussion

3.1. Preparation of seed latexes

Four series of PAEMA seed latexes were successfully synthesized by means of soap-free emulsion polymerization, with very little agglomerated material formed. PAEMA seed latex particles were cross-linked to varied degrees with EGDMA, except for AX0 in which case no cross-linker was added. The prepared latex particles were all relatively monodispersed with number-average diameters of 398.9, 313.6, 308.0 and 318.2 nm for AX0, AX0.5, AX1.0 and AX4.0, respectively, as determined by DLS analysis. A marked increase in diameter for AX0 is evident in comparison with others, due primarily to the higher ratio of monomer/water (cf. Table 1) originally charged to the reactor [33–37]. Also, within experimental error, particle sizes are likely to be independent of the cross-linking level when other polymerization conditions were held constant. It should be pointed out, however, in the solubility experiments to confirm the exact network formation in seed particles, AX0 was unexpectedly found not to dissolve in the common solvent such as THF and DMF, similar to AX0.5, AX1.0 and AX4.0. This insolubility indicates that the virtual network was formed to some extent even in AX0, presumably owing to the entanglement of polymer chains or chain transfer reaction. Accordingly, the two-stage latex particles prepared with AX0 seed were also referred to LIPN in this study.

3.2. Growth of latex particles during the second-stage polymerization

The particle size distribution curves by DLS analysis for AX1.0 and LIPNs prepared with AX1.0, as shown in Fig. 1, provided a good picture with regard to the growth of the latex particles during the second-stage soap-free emulsion polymerization. The increase in the amount of styrene monomer added in the second-stage polymerization increased the resultant particle size with no distinct change in size distribution. Additionally, in every sample of LIPNs, the formation of new crop of particles was not recognized. This suggests that the number of seed latex particles used according to the present polymerization conditions was sufficient to capture all the oligomeric radicals generated in

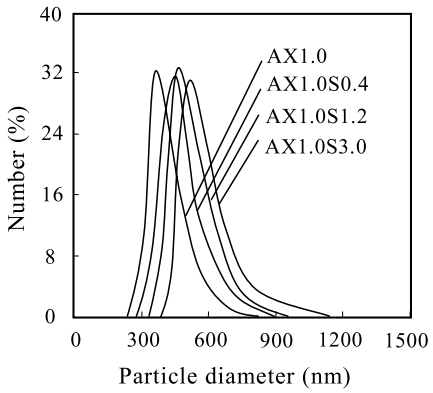

Fig. 1. Particle size distributions determined by DLS analysis for AX1.0 seed and PAEMA/PS LIPNs.

the aqueous phase so that the secondary nucleation of styrene was successfully avoided [38].

3.3. Bulk and surface compositions of LIPNs

The bulk composition of LIPN particles, in mol% of styrene unit, was determined by IR measurements. Typical IR spectra of AX1.0 and AX1.0S1.2 are shown in Fig. 2. For AX1.0, characteristic absorption peaks due to CH_3 bending, C=O stretching and acetic ester stretching vibration [39] were observed at about 1377, 1740 and 1234 cm^{-1}, respectively. As compared with AX1.0, some new absorptions such as those near 700 and 3026 cm^{-1} appeared in the IR spectrum of AX1.0S1.2, which could be reasonably assigned to the characteristic absorptions of aromatic C–H bending and aromatic C–H stretching vibrations. These results indicate that PS component was successfully introduced into the AX1.0 seed particles. The characteristic absorptions at 700 cm^{-1} for PS and at 1375 cm^{-1} for PAEMA were chosen to evaluate the bulk composition of LIPNs applying Lambert–Beer law. The corresponding molar absorptivities determined preliminarily in this laboratory are 12.2 and 6.5 $m^2\ mol^{-1}$, respectively.

The surface composition of LIPN particles was quantified by XPS analysis. According to the respective number of carbon and oxygen atom present in AEMA and styrene molecule, an equation was derived by a mathematical method

$$S\ \text{mol\%} = \left(1 - 2\frac{\text{O}}{\text{C}}\right) \times 100$$

where S mol% is the surface composition being required, in terms of mol% of styrene unit, and O/C is the atomic ratio of oxygen to carbon, which can be obtained from the multi-measurement of XPS. In our present study, all XPS measurements were made at a take-off angle of 45°. This enabled the analysis of the top particle surface with a few nanometers depth.

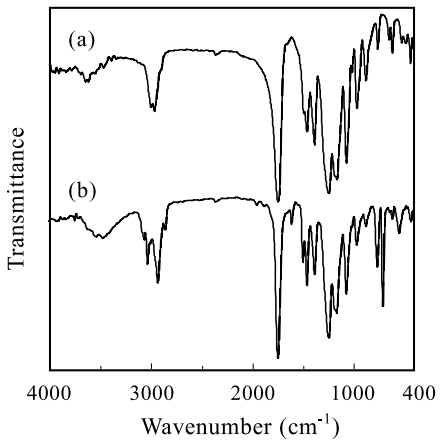

Fig. 2. IR spectra of (a) AX1.0; and (b) AX1.0S1.2 LIPN.

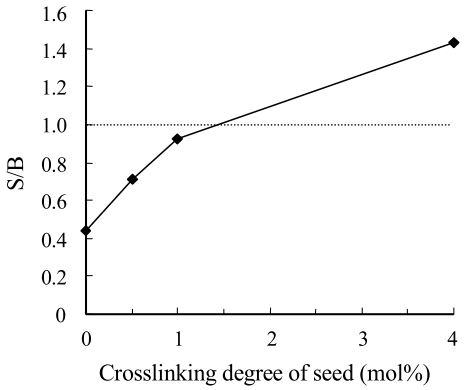

Fig. 3. Distribution of PS phase within PAEMA/PS LIPN particles.

The surface and bulk composition of PAEMA/PS LIPN particles are summarized in Table 3. For AX1.0S0.4, AX1.0S1.2 and AX1.0S3.0, which were all prepared by using the same AX1.0 seed, the PS contents in surface and bulk were found to be very close. This indicates that the PS phase is likely to distribute the LIPN particles throughout uniformly. However, the LIPN particles seem to become fairly heterogeneous in composition as the cross-linking degree of seed particles was either reduced or increased; this can be seen more directly from Fig. 3 in which the ratio of the surface composition to bulk composition (S/B) were plotted versus the cross-linking degree of the seed particles. In contrast to AX1.0S1.2, which gives a S/B value near unity, both AX0S1.2 and AX0.5S1.2 assume the S/B values smaller than unity, whereas AX4.0S1.2 assumes a value larger than unity. From these results, it should be concluded

Table 3
Bulk and surface compositions of PAEMA/PS LIPN particles

LIPNs	Bulk composition (mol%)	Surface composition (mol%)
AX1.0S0.4	23.8	22.2
AX1.0S1.2	45.5	41.9
AX1.0S3.0	74.4	73.5
AX0S1.2	40.7	17.8
AX0.5S1.2	42.5	30.3
AX4.0S1.2	43.6	62.5

In terms of mol% of styrene unit.

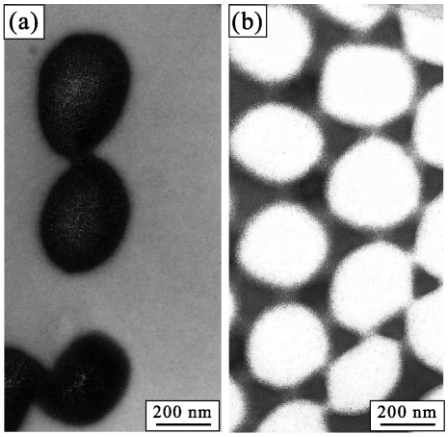

Fig. 4. Transmission electron micrographs of (a) PS; and (b) AX1.0 latex particles prepared by soap-free emulsion polymerization. Both samples were stained with RuO_4 vapor.

that there may exist a compositional gradient from the center to the surface within LIPN particles, with the majority of PS component localizing near the particle center for AX0S1.2 and AX0.5S1.2, and, inversely, near the surface for AX4.0S1.2.

3.4. Internal morphology of LIPN particles

TEM observation was carried out on RuO_4-stained ultrathin cross-sections to examine the internal morphology of LIPN particles. As opposed to the fact that the RuO_4 vapor can readily stain PS polymer to a great extent [40,41], this staining agent was found to be extremely inactive to PAEMA polymer. Fig. 4 shows a comparison of AX1.0 (ϕ: ca. 308 nm) and PS (ϕ: ca. 300 nm) latex particles examined under the completely same microtome and staining technique; the PS latex particles were prepared by the similar polymerization procedure as AX1.0. Both AX1.0 and PS appear structureless, with AX1.0 being light and PS dark. This observation confirms that the RuO_4-staining technique used in this study is sufficient to provide adequate morphological contrast between PAEMA and PS phase within PAEMA/PS LIPN particles. In addition, during TEM observation of PAEMA/PS LIPN particles, no PS particles were found; such particles would have been distinguished as dark image similar to that shown in Fig. 4(a). This suggests that no new nucleation of styrene monomer occurred during the second-stage polymerization, which coincides with the results of DLS analysis.

3.4.1. Effect of cross-linking degree of seed particles

Fig. 5 gives the transmission electron micrographs of the PAEMA/PS LIPNs that were prepared with PAEMA seeds cross-linked to different degrees. PS contents in these LIPNs are ca. 42 mol% (cf. Table 3). All LIPNs have a microphase-separated structure and the light PAEMA-rich phase is believed to constitute the continuous phase, in which the darkly stained PS-rich phase disperses. Although they seem to be somewhat semi-continuous and thus complicate the quantification, PS-rich domain sizes are evidently decreased as the cross-linking degree of PAEMA seeds increased from 0 to 4 mol%, which is clear from the comparison of Fig. 5(a)–(d). In addition, it is apparent from Fig. 5(d) that nearly all of the PS-rich phase exists at the periphery of particle, forming the so-called core/shell morphology. This is in good agreement with the compositional analysis. The localization of PS component at the particle surface can also be seen from the smaller particle in Fig. 5(d), which was sliced from the outer edge of particle and gives an almost uniform distribution of PS-rich phase.

The decrease of the phase domain size with increasing cross-linking density, especially of the first-stage polymer, was also reported with respect to the bulk sequential IPN [42–45]. This may be related to the increased restriction on the mobility of growing polymeric chains due to the first-stage polymer network. The highly cross-linked network in which the effective mean chain length between cross-links is extremely small compared to the slightly cross-linked network, may further retard or prevent the second-stage polymer chains from diffusing into the already existing network of first-stage polymer [46]. As a result, the phase separation is prohibited and degree of interpenetration of two polymer components improved; in some cases, a homogeneous IPN can be obtained.

However, it must be noted that the distribution of PS-rich phase within PAEMA-rich matrix is rather uniform for both AX0S1.2 and AX0.5S1.2 particles (Fig. 5(a) and (b)), practically consistent with the appearance of AX1.0S1.2 particles (Fig. 5(c)). This is a result at variance with the analysis of bulk and surface compositions and is presumed to be the artifacts originating from the embedding procedure. As will be described later in this paper, the ultimate LIPN morphology is determined by the combined effect of particle/water interfacial tension and local viscosity of polymerization loci at reaction temperature. When the LIPN particles were embedded in epoxy resin during the curing procedure at 60 °C, the environment of the particles altered from water to epoxy resin which has a much less polarity than the former. As a consequence, the hydrophobic PS-rich phase, having relatively high mobility in the weakly cross-linked AX0S1.2 and AX0.5S1.2, might migrate towards the particle surface in order to establish a new balance between interfacial tension and intraparticle viscosity.

3.4.2. Effect of composition

AX1.0S0.4, AX1.0S1.2 and AX1.0S3.0 LIPNs prepared using identical AX1.0 seed were chosen to clarify the effect of composition. As the addition amount of styrene was increased from 0.4 to 1.2 ml, which doubled the PS bulk content in the resultant LIPN (cf. Table 3), the increase of PS-rich phase within PAEMA-rich matrix is observed and the size of PS-rich domains remains roughly unchanged, as shown by the comparison of Figs. 6(a) and 5(c). On the other

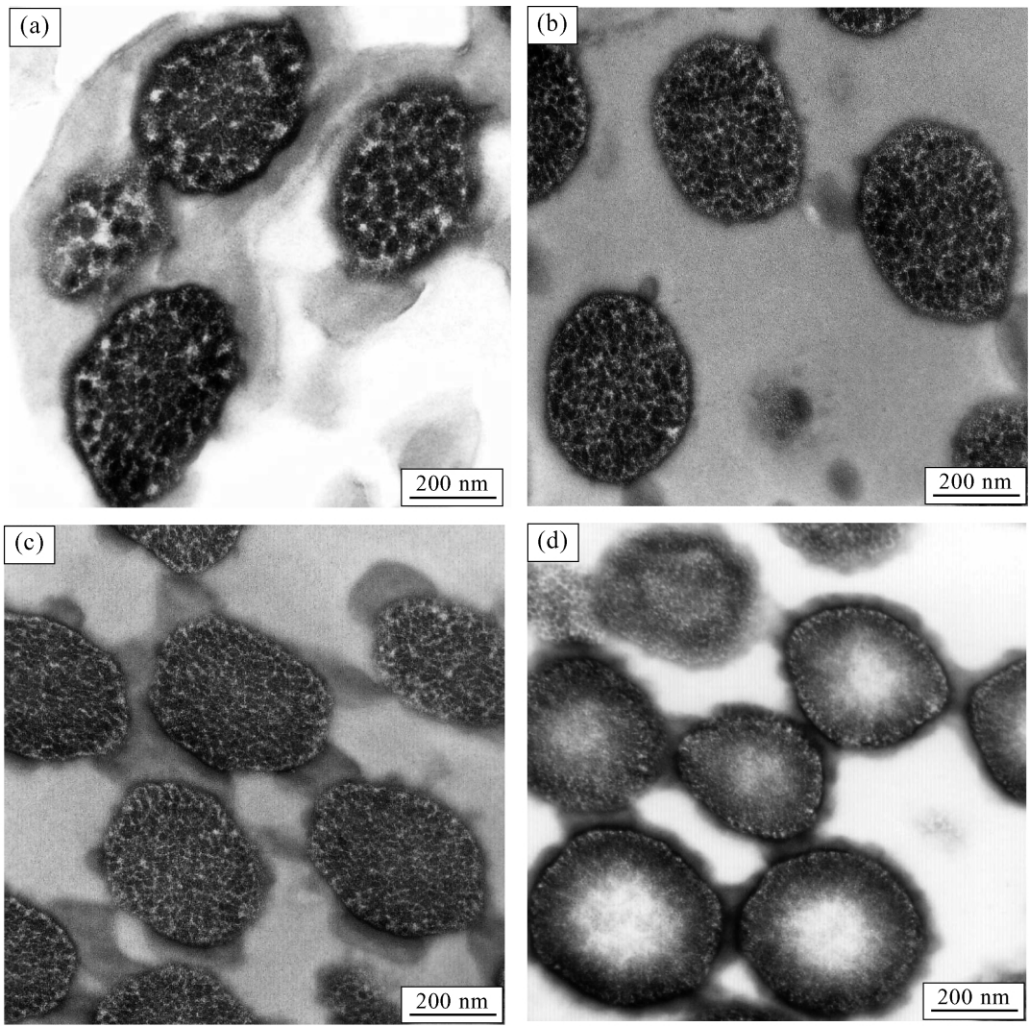

Fig. 5. Transmission electron micrographs of PAEMA/PS LIPN particles: (a) AX0S1.2; (b) AX0.5S1.2; (c) AX1.0S1.2; and (d) AX4.0S1.2. PS phase was stained dark with RuO_4 vapor.

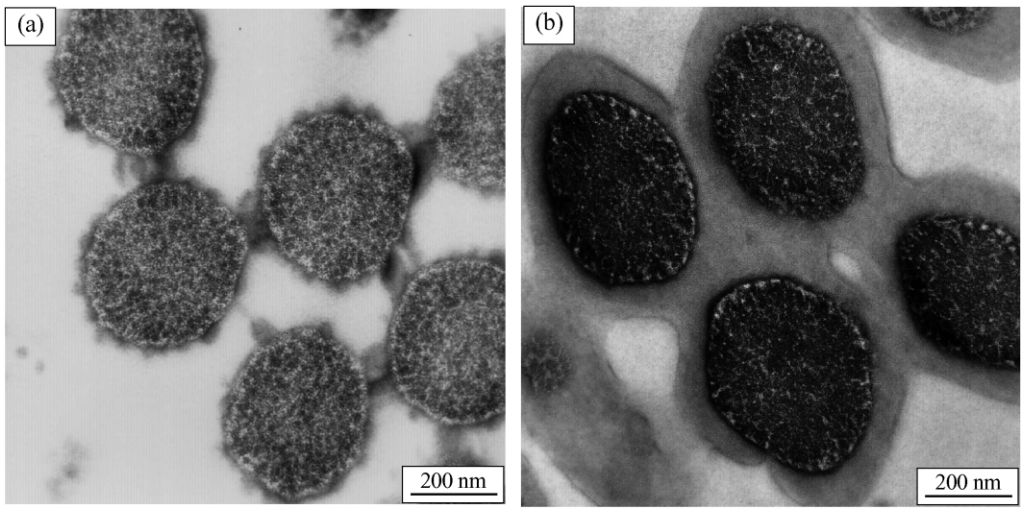

Fig. 6. Transmission electron micrographs of (a) AX1.0S0.4; and (b) AX1.0S3.0 LIPN particles. PS phase was stained dark with RuO_4 vapor.

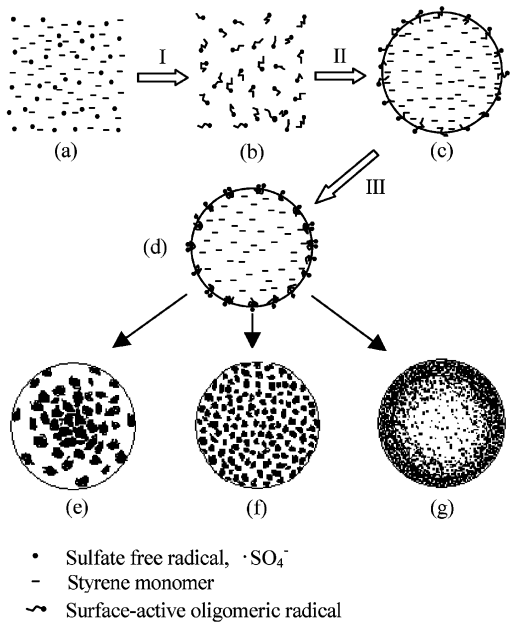

Fig. 7. Schematic representation of the particle growth mechanism for the second-stage soap-free emulsion polymerization.

hand, further increase of styrene addition amount to 3.0 ml seems likely to result in the occurrence of phase inversion, with PS-rich phase becoming continuous and PAEMA-rich phase dispersed, as shown in Fig. 6(b). The above observations on electron micrographs also confirm the uniform distribution of PS-rich phase over the entire particle, throughout the range of compositions, thus in accordance with the compositional analysis.

3.5. Particle growth mechanism

The second-stage soap-free emulsion polymerization was suggested to proceed in the following three steps:

(I) Formation of the surface-active oligomeric radicals in water phase.
(II) Adsorption of the surface-active oligomeric radicals onto the interface of monomer-swollen particle and water.
(III) Chain propagation in the interface with subsequent phase migration.

This particle growth mechanism is depicted schematically in Fig. 7.

The thermal decomposition of water-soluble initiator, KPS, generates the primary sulfate free radicals, SO_4^- [47,48]. These sulfate radicals then react with styrene monomer marginally dissolved in the aqueous phase to form surface-active oligomers with a critical chain length of z (Fig. 7(b)). At 70 °C, the value of z, i.e. the number of styrene units, can be calculated to be approximately within the range of 2–4 by applying the equations proposed by Maxwell et al. [49]. The surface-active oligomeric radicals thus created are instantaneously captured by the monomer-swollen particles, with polar SO_4^- end groups remaining in the aqueous phase and short hydrocarbon chains located in the monomer-swollen particle/water interface (Fig. 7(c)). In the interface, the hydrocarbon end of the newly generated oligomeric chain, to which the radical activity has been transported from the sulfate groups, encounters a high concentration of monomer and rapid chain propagation occurs (Fig. 7(d)).

As the chain propagation proceeds, the surface-active oligomeric radicals lose their surface-activity and become hydrophobic. Such newly formed second-stage polymer (or polymeric radicals) would show a strong tendency to penetrate into the particle interior so as to form the hydrophilic PAEMA/water interface instead of hydrophobic PS/water interface, to minimize the interfacial free energy and become more thermodynamically stable [50,51].

However, when the hydrophobic PS phase migrates towards particle center, a kinetic resistance emerges which arises from the internal particle viscosity determined mainly by the cross-linking level at present system. Accordingly, the final morphology of the resulting LIPN particles is simultaneously and competitively controlled by the interfacial tension and local particle viscosity, the former acting as thermodynamic driving force for phase migration and the latter as kinetic resisting force to above process. For the weakly cross-linked AX0S1.2 and AX0.5S1.2, the thermodynamic influence may predominate and the morphology of PS component mainly existing near the particle center resulted (Fig. 7(e)); on the other hand, for highly cross-linked AX4.0S1.2, the kinetic influence might prevail over the thermodynamic one and most PS components were restricted to the particle surface (Fig. 7(g)). When styrene was polymerized on AX1.0 seed particles, the thermodynamic and kinetic factors tend to commensurate, hence forming the particle morphology with PS component distributed uniformly (Fig. 7(f)). Of course, the high viscosity of polymerization locus limits the behavior of not only phase migration but also phase separation, resulting in the finer PS-rich domains. This has been described in Section 3.4.

4. Conclusion

A series of PAEMA/PS LIPNs were prepared by polymerizing styrene monomer on the submicron-size PAEMA seed particles. From the characterization of bulk and surface compositions, it was found that the distribution of PS phase within LIPN particles could be controlled by altering the degree of cross-linking of PAEMA seed particles. In addition, all PAEMA/PS LIPNs were microphase-separated, with PS-rich domains appearing larger for lightly cross-linked LIPNs and extremely finer for highly cross-linked one. The microphase-separated structure was observed to be present even at the surface of PAEMA/PS LIPN particles. To explain the observed results, a particle

growth mechanism containing the water phase formation of surface-active oligomeric radicals, adsorption of the surface-active oligomeric radicals onto the monomer-swollen particle/water interface and rapid chain propagation in the interface with subsequent phase migration process was proposed.

Acknowledgements

The authors would like to thank Prof. T. Komoto of Gunma University for his helpful discussion and technical support during the observation of electron microscopy.

References

[1] Manson JA, Sperling LH. Polymer blends and composites. New York: Plenum Press; 1976. Chapter 8.
[2] Sperling LH, Chiu TW, Gramlich RG, Thomas DA. J Paint Technol 1974;46:47.
[3] Grates JA, Thomas DA, Hickey EC, Sperling LH. J Appl Polym Sci 1975;19:1731.
[4] Silverstein MS, Narkis M. Polym Engng Sci 1985;25:257.
[5] Silverstein MS, Narkis M. J Appl Polym Sci 1987;33:2529.
[6] Hourston DJ, Satgurunathan R. J Appl Polym Sci 1984;29:2969.
[7] Hourston DJ, Satgurunathan R, Varma H. J Appl Polym Sci 1986;31: 1955.
[8] Hourston DJ, Satgurunathan R, Varma HC. J Appl Polym Sci 1987; 34:901.
[9] Lee DI, Ishikawa T. J Polym Sci, Polym Chem Ed 1983;21:147.
[10] Sperling LH, Chiu TW, Thomas DA. J Appl Polym Sci 1973;17:2443.
[11] Lee S, Rudin A. J Polym Sci, Polym Chem 1992;30:2211.
[12] Burford RP, Vo CD. J Appl Polym Sci 1999;74:629.
[13] Lee JS, Shin JH, Kim BK, Kang YS. Colloid Polym Sci 2001;279:959.
[14] Hourston DJ, Satgurunathan R, Varma H. J Appl Polym Sci 1987;33: 215.
[15] Hourston DJ, Romaine J. J Appl Polym Sci 1990;39:1587.
[16] Wang JY, Liu RY, Li WH, Li WY, Tang XY. Polym Int 1996;39:101.
[17] Dickie RA, Cheung MF, Newman S. J Appl Polym Sci 1973;17:65.
[18] Lee CF, Chiu WY. J Appl Polym Sci 1997;65:425.
[19] Hourston DJ, Romaine J. Eur Polym J 1989;25:695.
[20] Durant YG, Sundberg EJ, Sundberg DC. Macromolecules 1997;30: 1028.
[21] Sperling LH, Chiu TW, Hartman CP, Thomas DA. Int J Polym Mater 1972;1:331.
[22] Nemirovski N, Silverstern MS, Narkis M. Polym Adv Tech 1996;7: 247.
[23] Montheard JP, Chatzopoulos M, Chappard D. JMS-Rev Macromol Chem Phys 1992;C32(1):1.
[24] Crulke EA. In: Brandrup J, Immergut EH, Grulke EA, editors. Polymer handbook, 4th ed. New York: Wiley; 1999. p. VII/707.
[25] Coleman MM, Graf JF, Painter PC. Specific interactions and the miscibility of polymer blends. Lancaster: Technomic; 1991. Chapter 2.
[26] Murayama S, Kuroda S, Osawa Z. Polymer 1993;34:2845.
[27] Murayama S, Kuroda S, Osawa Z. Polymer 1993;34:3893.
[28] Kawaguchi H, Hoshino H, Amagasa H, Ohtsuka Y. J Colloid Interf Sci 1984;97:465.
[29] Kamel AA, Ma CM, El-Aasser MS, Micale FJ, Vanderhoff JW. J Dispersion Sci Technol 1981;2:315.
[30] Matsumoto T, Ochi A. Kobunshi Kagaku 1965;22:481.
[31] Noma H, Tanba S, Iida S, Nakasato Y. Kobunshi Ronbunshu 1975;32: 189.
[32] Trent JS. Macromolecules 1984;17:2930.
[33] Goodwin JW, Hearn J, Ho CC, Ottewill RH. Colloid Polym Sci 1974; 252:464.
[34] Zhou DZ, Aklonis JJ, Salovey R. J Polym Sci, Polym Chem 1992;30: 2443.
[35] Härtl W, Zhang-Heider X. J Colloid Interf Sci 1997;185:398.
[36] Koenderink GH, Sacanna S, Pathmamanoharan C, Rasa M, Philipse AP. Langmuir 2001;17:6086.
[37] Tanrisever T, Okay O, Sonmezoglu IC. J Appl Polym Sci 1996;61: 485.
[38] Fitch RM, Shih LB. Prog Colloid Sci 1975;56:1.
[39] John RD. Applications of absorption spectroscopy of organic compounds. New Jersey: Prentice-Hall; 1965.
[40] Trent JS, Scheinbeim JI, Couchman PR. J Polym Sci. Polym Lett Ed 1981;19:315.
[41] Trent JS, Scheinbeim JI, Couchman PR. Macromolecules 1983;16: 589.
[42] Sperling LH. In: Klempner D, Sperling LH, Ultracki LA, editors. Interpenetrating polymer networks. Advances in chemistry series, 239. Washington, DC: American Chemical Society; 1994. Chapter 1.
[43] Donatelli AA, Sperling LH, Thomas DA. Macromolecules 1976;9: 671.
[44] Donatelli AA, Sperling LH, Thomas DA. J Appl Polym Sci 1977;21: 1189.
[45] Kotaka T, Nishi S, Adachi H. In: Klempner D, Frisch KC, editors. Advances in interpenetrating polymer networks, vol. 2. Lancaster: Technomic; 1989.
[46] Meseguer Duenas JM, Torres Escuriola D, Gallego Ferrer G, Monleon Pradas M, Gomez Ribelles JL, Pissis P, Kyritsis A. Macromolecules 2001;34:5525.
[47] Bartlett PD, Cotman Jr. JD. J Am Chem Soc 1949;71:1419.
[48] Kolthoff IM, Miller IK. J Am Chem Soc 1951;73:3055.
[49] Maxwell IA, Morrison BR, Napper DH, Gilbert RG. Macromolecules 1991;24:1629.
[50] Sundberg DC, Casassa AP, Pantazopoulos J, Muscato MR. J Appl Polym Sci 1990;41:1425.
[51] Sundberg DC, Durant YG. NATO ASI Ser, E 1997;335:177.